

# First Results of Project on Six-hourly EOP Piecewise Linear Offset Parameterization

A. Nothnagel<sup>1</sup>, S. Böhm<sup>1</sup>, R. Dach<sup>2</sup>, M. Glomsda<sup>3</sup>, H. Hellmers<sup>4</sup>, A.-S. Kirkvik<sup>5</sup>, T. Nilsson<sup>6</sup>, A. Girdiuk<sup>4</sup>, D. Thaller<sup>4</sup>

**Abstract** Continuous piecewise linear functions are a helpful way of parameterizing time series in least-squares adjustments employing a Gauss-Markov model. In this publication, we present the benefits for routine IVS Earth Orientation Parameter (EOP) estimation and show results of a project set up for demonstrating the feasibility of this approach. Before we start with that, we point out deficits of the current EOP estimation approach with 24-hour offsets and rates stemming from the mismatch of tabulated a priori EOP values at day boundaries and the two-calendar-day spanning of contemporary IVS observing sessions. In addition, the current EOP parameterization causes a mismatch of the IVS-derived EOPs labeled with “24 hours” with the daily EOPs derived from other space-geodetic techniques.

**Keywords** Earth Orientation Parameter estimation, continuous piecewise linear functions

## 1 Introduction

In routine Earth Orientation Parameter (EOP) estimation of the International VLBI Service for Geodesy

and Astrometry (IVS) functional values at a reference epoch (commonly called offset) and the first time derivative (commonly called rate) are the parameters of interest for the two polar motion (PM) components  $x_p$  and  $y_p$  as well as for universal time represented as UT1-UTC. For the latter parameter, the rate reflects the length of day (LOD) which has the opposite sign for historical reasons. In terms of consistent handling of multiple solutions of different IVS Analysis Centers (ACs), the use of identical a priori values for every individual delay observation is a fundamental prerequisite.

The current procedure is that EOP tables of the International Earth Rotation and Reference Systems Service (IERS) are used: either the tables of the IERS Rapid Service and Predictions Center (usno\_finals) or the IERS Series C04. Both contain time series of EOP at midnight epochs with daily resolution. These are then taken to interpolate the respective EOP components at the epoch of the delay observation either linearly, as spline functions, or with the Lagrange method. With the individual EOP at time of observation, the observed-minus-computed vector is corrected for the variability in Earth rotation. Furthermore, the set of EOP values at the session’s reference epoch, normally the middle of the session, is calculated for the computation of the total unknown parameters composed of these a priors and the adjustments.

The critical part is related to the EOP rates and their a priors. What happens here is dependent on the EOP reference epoch of the session. Since most IVS observing sessions start around 18h00 UT, the EOP reference epoch is at around 06h00 UT and thus between the second and third midnight epoch used for interpolation (Figure 1). In most analysis software packages, the a priori EOP rate is then calculated with these second

1. Technische Universität Wien, Department für Geodäsie und Geoinformation, Wiedner Hauptstraße 8, 1040 Wien, Austria

2. University of Bern, Astronomical Institute, Switzerland

3. Deutsches Geodätisches Forschungsinstitut der Technischen Universität München (DGFI-TUM), Germany

4. Federal Agency for Cartography and Geodesy (BKG), Frankfurt a.M., Germany

5. Norwegian Mapping Authority (NMA), Kartverksveien 21, 3511 Hønefoss, Norway

6. Lantmäteriet – The Swedish mapping, cadastral and land registration authority, Lantmäterigatan 2C, 801 82 Gävle, Sweden

and third functional values (rate II) depending on the interpolation scheme. As is obvious from Figure 1, this rate does not represent the real EOP rate for the whole observing session but only that of the last 3/4 of the total session length. If the session lasts from 18h00 UT to 18h00 UT as in Figure 1, the correct a priori rate would be the one which is depicted as rate III. The effect on the total EOP estimate, i.e., a priori plus adjustment, may be small for polar motion rates, but may be significant for LOD.

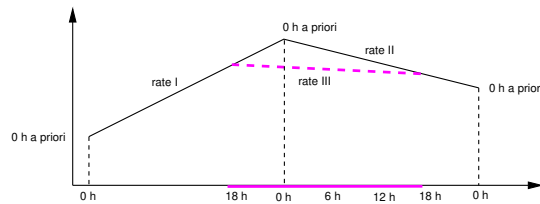


**Fig. 1** Current scheme of EOP interpolations from IERS tables. In magenta, the correct rate representation for a generic observing session from 18h00 UT to 18h00 UT is depicted. Linear interpolation is chosen for a good interpretability of the graph, but the same applies also for any other interpolation scheme.

Another issue in this context is the documentation of the a priori rates in the SINEX files. Usually, there is no indication of what a priori rates are reported, so the parameter epoch transformation in the combination process at the IVS Combination Center is applied without distinction.

Furthermore, this kind of EOP parameterization results in estimates that are labeled as “24-hour EOPs,” but the 24-hour interval is fully different from the 24-hour intervals for EOP estimation by the other space-geodetic techniques, which is usually attached to the standard day, i.e., covering 00h00 UT to 24h00 UT [7]. As a consequence, these EOPs cannot be reliably combined, although it is still done for the operational IERS EOP products.

To overcome these deficits in IVS operations and prepare for a higher time resolution of EOP in the VGOS era, we propose to establish routine EOP estimation with continuous piecewise linear functions (CPLF) at fixed intervals and epochs. CPLFs come along in two different representations: with rates, or with functional values at supporting points (Figure 2). In the first case, the estimated parameters are an offset or functional value  $f_0$  at a reference epoch (e.g., at the start of the session) and a series of new rates  $r_i$  for con-

secutive intervals continuously linked together at the nodes. Mathematically equivalent is the estimation of a series of functional values  $f_i$  for the nodes.

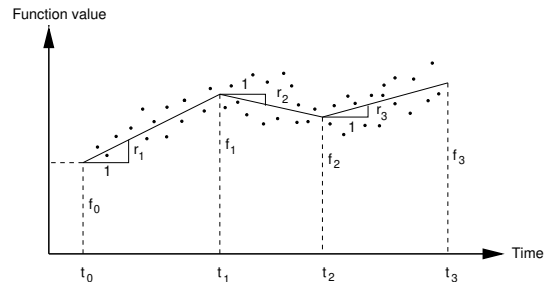


**Fig. 2** Continuous piecewise linear function fit to generic observations (dots) either with an initial functional value  $f_0$  and a series of rates  $r_i$ , or with a series of functional values  $f_i$  for the nodes.

Applying this scheme to EOP estimation for IVS EOP observing sessions allows to increase the time resolution easily, and permits the reporting of unambiguous a priori values of the nodes as interpolated from the tabulated IERS values at midnight epochs (Figure 3) in the SINEX files. Ideal is the choice of nodes at fixed integer hours including the midnight epoch, e.g., 18h00 UT, 00h00 UT, 06h00 UT, 12h00 UT, and 18h00 UT for six-hour intervals. In doing so, the resulting EOPs can easily and unambiguously be compared and combined with EOPs resulting from the other space-geodetic techniques.

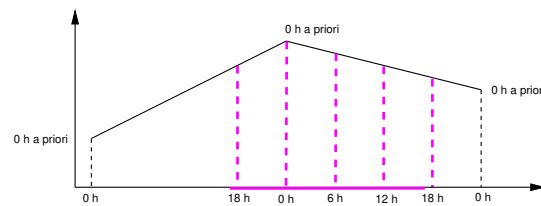


**Fig. 3** Proposed scheme of EOP interpolations from IERS tables. In magenta, the nodes at six-hourly intervals (including 0h00 UT) for a generic observing session from 18h00 UT to 18h00 UT is depicted. Linear interpolation is chosen for a good interpretability of the graph, but the same applies also for any other interpolation scheme.

## 2 Experiment Setup

To demonstrate the validity of the concept, we performed a test by analyzing all 52 IVS-R1 sessions of

the year 2020 with six-hourly continuous piecewise linear offsets. The level 2 data analysis was carried out with the softwares ASCoT (OSO) [1], (Calc/Solve, not invertible), DOGS-RI (DGF) [6], Where (NMA) [5], and VieVS (VIE) [2], with the standard setup as used in the computations for the ITRF2020 submissions. Due to the observing periods of the R1 sessions from 17h00 to 17h00 UT, we estimated the Earth Rotation Parameters (ERP) at 12h00, 18h00, 0h00, 6h00, 12h00, and 18h00 UT, covering the observing session in its entirety. Since the first section (12h00 to 18h00 UT) merely contains observations of one hour (17h00 to 18h00 UT), the first parameter of each session is determined only very weakly. Therefore, we excluded these parameters in the subsequent interpretations.

In the simultaneous estimation of polar motion and celestial pole offsets (CPO), the higher the time resolution of polar motion, the more correlated the corresponding estimates are. Hence, we fixed the CPOs to the IAU2000A/2006 nutation model plus an empirical Free Core Nutation (FCN) model (Section 3). Furthermore, all sub-daily geophysical models were organized to be identical.

For our assessment, we also made use of combined time series produced by the IVS Combination Center at BKG in the same way as those for ITRF2020 [4]. The combination could be performed straight away with no major modifications of the combination software necessary. The combined time series then formed an additional ERP data set.

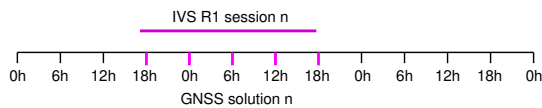


**Fig. 4** Extraction scheme of GNSS results.

To allow for an external comparison, a special CODE Analysis Center GNSS solution [3] was computed with the same six-hourly resolution as for the VLBI solutions. For stability reasons, three-day arcs with 13 ERP epochs were chosen, where the terrestrial frame was estimated session-wise with No-Net-Rotation conditions w.r.t. IGS3. This setup allowed the extraction of consistent ERP from a single three-day arc for epochs identical to the six VLBI session epochs (Figure 4).

### 3 Handling of Nutation

It is well known that the separation of polar motion and celestial pole offsets is only possible through the concept of a rotation axis. We need a full rotation of the Earth to decorrelate PM and CPOs sufficiently. VLBI observations at a single epoch alone will only have three rotational degrees of freedom and the normal equation system will be singular if we set up both PM and CPO parameters in this case. The more time of a day we cover with observations, the more the correlation coefficients between PM and CPOs will be reduced. In the opposite direction, we face higher and higher correlations when we introduce more and more continuous piecewise linear offsets (PWLO). This has an effect already for six-hour intervals, and therefore the estimation will require some constraints on the CPOs to detect genuine signals in the PWLOs for PM.

The standard procedure is to take the IERS 14C04 or a VLBI solution's CPOs and interpolate between adjacent epochs with some suitable interpolation scheme. However, the VLBI results for the CPOs, which are the basis for IERS 14C04 or usno\_finals, are rather noisy by several tens of microarcseconds from session to session. On one hand, there is no nutation variability below two days by the IERS PM/CPO conventions. On the other hand, the main phenomenon which should dominate the CPO estimates is FCN, with variable amplitudes up to 0.3 mas and a more or less constant period of 430 days. Although there might be a retrograde resonance of Atmospheric Angular Momentum in the FCN band, time series analyses of the CPOs do not show unmodeled effects larger than 30  $\mu$ as (Ferrándiz, priv. comm.). Any interpolation scheme for fixing the CPOs will thus only generate noise in the PM data.

Since FCN is the dominant variation in the CPOs, we fitted the parameters of a simple 430-day period sine/cosine function (plus rate and offset) to the VLBI data from 2019/07/01 to 2021/06/30 (Figure 5) to cover the year 2020 with some overlap and about two FCN periods. The quality of the fit should then just be assessed by the data in 2020. The residuals are still quite large which underscores that the accuracy of the VLBI CPO estimates is only about 80–100  $\mu$ as. The model for any Modified Julian Day (MJD) epoch is

$$\text{comp [mas]} = A \cdot \sin(f \cdot t) + B \cdot \cos(f \cdot t) + C + D \cdot t \quad (1)$$

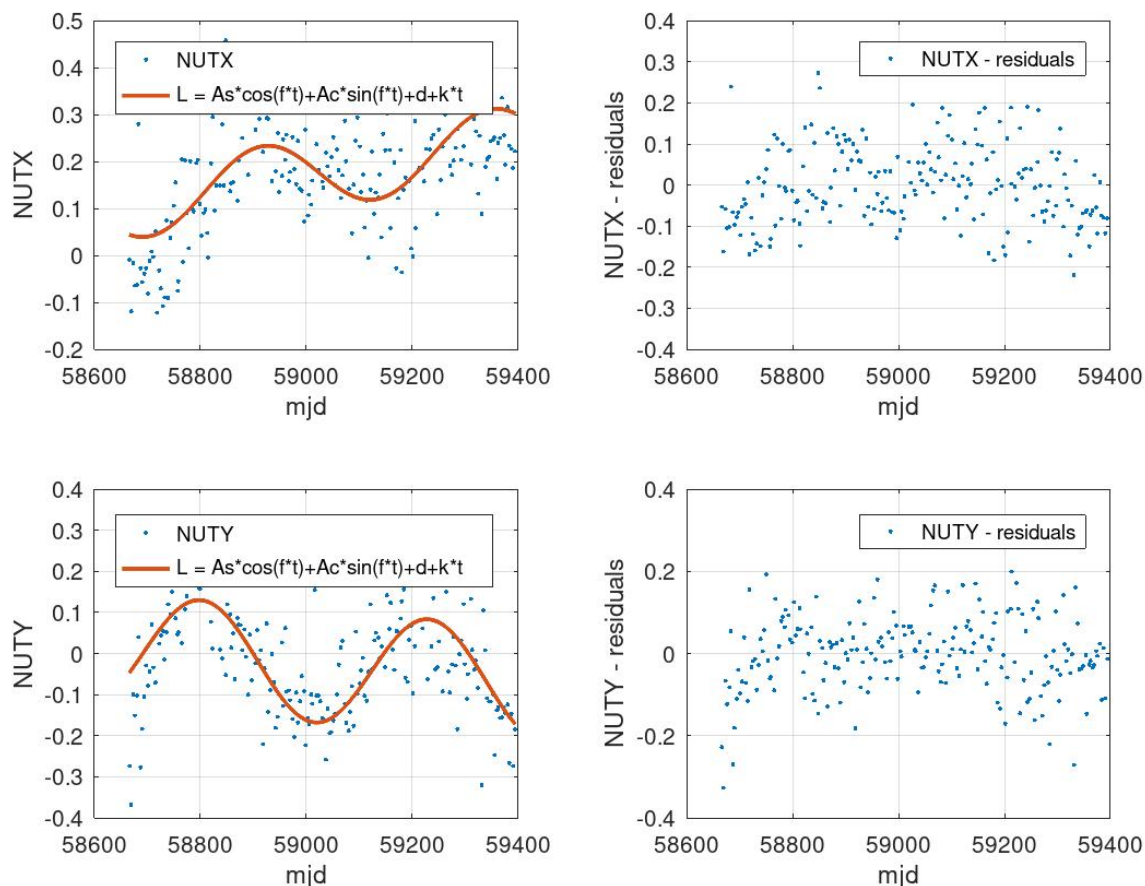


**Fig. 5** Estimation of Free Core Nutation from  $dX/dY$  celestial pole offsets. Left: Observations with fit ( $L$ ) in red. Right: Residuals of fit. All in mas.

with frequency  $f = 2\pi/430$  and epoch  $t = MJD - 58849.0$ . The estimated coefficients for the  $X$  nutation component are  $A = +0.06373$  mas,  $B = +0.04188$  mas,  $C = +0.14386$  mas, and  $D = +0.00018$  mas/day. For the  $Y$  nutation component, they are  $A = -0.08826$  mas,  $B = +0.10496$  mas,  $C = -0.01245$  mas, and  $D = -0.00011$  mas/day. These were used to compute the fixed CPOs for each MJD, and the results are added to the IAU2000A/2006 nutation components in the VLBI analyses of all ACs.

## 4 Results

The first analysis step was a direct comparison of the estimates from the individual ACs, which revealed a few inconsistencies in modeling and general setup. After eliminating these, it turned out that 15 of the IVS R1 sessions had an insufficient number of telescopes par-

ticipating, especially in the second half of 2020. Consequently, the number of observations per six-hour interval was rather small, leading to a larger than expected scatter in the ERP estimates. For the sake of easy implementation, a general threshold of a minimum number of stations of nine was introduced. At this stage, we did not test any other minimum criterion. This is foreseen for future steps of the project.

The scatter of the results of individual sessions and of individual Analysis Centers can best be depicted if an offset and a rate, as regularly estimated for each session in standard VLBI analyses, are subtracted from the PWLO estimates. With at least nine telescopes participating in every R1 session, the general variability of all individual VLBI solutions, their combination, and also the GNSS results is approximately  $\pm 500 \mu\text{as}$  for  $x$  pole (Figure 6); the  $y$  pole component is similar.

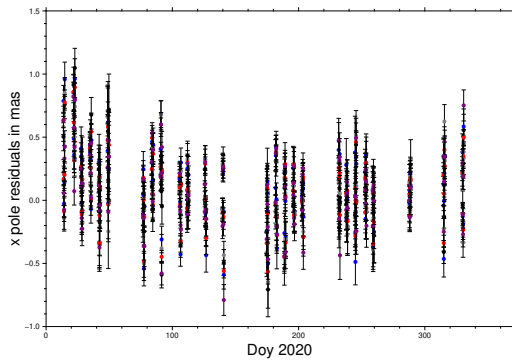


**Fig. 6**  $x$  pole component variability in each session. Black = VIE, Light Blue = NMA, Gray = OSO, Dark Red = DGF, Blue = GNSS, Red = VLBI Combi.

In terms of agreement between VLBI and GNSS, the WRMS differences of all ACs are in the range of 250 to 300  $\mu\text{s}$ , with the  $x_p$  component agreeing slightly better (Table 1).

**Table 1** WRMS of VLBI minus GNSS in  $\mu\text{s}$  ( $n$  = number of epochs = 130); 20  $\mu\text{s}$  bias subtracted in  $y_p$ .

|       | VIE | NMA | OSO | DGF | Combi |
|-------|-----|-----|-----|-----|-------|
| $x_p$ | 249 | 276 | 266 | 269 | 255   |
| $y_p$ | 286 | 296 | 281 | 282 | 277   |

Since the VLBI combination nicely represents all VLBI contributions, in the next steps only the VLBI combination results and the GNSS results are compared for a better graphical visualization (Figure 7 and zoom of the first six sessions of 2020 in Figure 8).

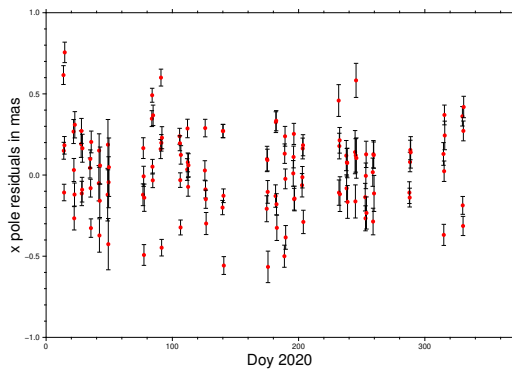


**Fig. 7**  $x$  pole component differences of VLBI combination minus GNSS.

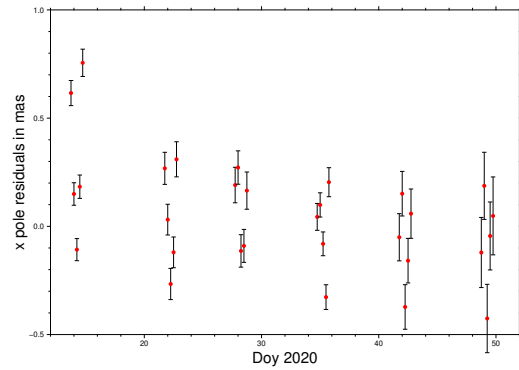


**Fig. 8**  $x$  pole component differences of VLBI combination minus GNSS, enlarged for first six sessions of 2020.

The plot of the differences of all sessions with nine or more telescopes (Figure 7) still looks rather arbitrary. Only when zooming in, some systematics show up. There seems to be an arc-like behavior with minima at or near the middle of the sessions. Since the differences between VLBI and GNSS should be random if both techniques produced correct results, the characteristics of the differences but also the results themselves need to be investigated further.

As a sideline of our investigations, we can also look at the differences of VLBI minus GNSS for the 0h UT epochs alone. In contrast to the routine VLBI–GNSS comparisons, no interpolation is needed for the VLBI results. However, the number of VLBI observations contributing to these parameters are naturally smaller in the PWLO case than for the operational offset and rate estimation from the full 24-hour sessions. Nevertheless, the results are rather promising (Table 2) since for the  $x_p$  component, they are about 20% smaller than the overall values (Table 1). Unfortunately, the differences of the  $y_p$  component are slightly larger. In any case, we can show that with the PWLO estimation the need for interpolations in VLBI–GNSS comparisons will disappear.

**Table 2** WRMS of VLBI minus GNSS for the 0h UT epoch alone in  $\mu$  ( $n$  = 26); no bias subtracted from  $y_p$  results.

|       | VIE | NMA | OSO | DGF | Combi |
|-------|-----|-----|-----|-----|-------|
| $x_p$ | 190 | 249 | 212 | 230 | 230   |
| $y_p$ | 303 | 313 | 307 | 319 | 303   |

## 5 Accuracy Considerations

The formal errors of the individual VLBI analyses are in the range of 100 to 200  $\mu\text{s}$  in all components. The combination produces formal errors in the range of 80 to 100  $\mu\text{s}$ . Although the GNSS results are reported with formal errors of 7 to 10  $\mu\text{s}$ , we know that we have to inflate them by a factor of about ten due to the neglect of correlations between subsequent carrier phase observations. The GNSS results can therefore be judged to be approximately of a similar quality as the VLBI combination results. The formal errors of the differences VLBI combi minus GNSS are then approximately 120  $\mu\text{s}$ , while the differences of the individual VLBI ACs minus GNSS are at the level of about 170  $\mu\text{s}$ . The scatter of the differences is thus by about 50% larger, as we see in the computed WRMS differences (Table 1).

## 6 Conclusions

In this paper we have demonstrated that estimating ERP with continuous piecewise linear functions with a temporal resolution higher than 24 hours can be realized easily by many VLBI ACs. This also applies to the combination process on the basis of normal equation systems. However, we also saw that robust networks with many observations per time interval are essential for this approach. The scatter of the differences between the VLBI and the GNSS results is still too large for a reliable interpretation of the results.

Nevertheless, the use of continuous piecewise linear functions with offset representation is the next step which the IVS analysis community has to go for a higher time resolution of the ERP results. In addition, this approach eliminates the deficit of incorrect handling of the a priori ERP rates when sessions extend across midnight epochs. Finally, unambiguous comparisons of ERP results from VLBI and other space geodetic techniques are possible without the need for interpolations, which regularly increase the noise level.

## References

1. T. Artz, S. Hallsig, A. Iddink, A. Nothnagel. ivg::ASCOT: Development of a New VLBI Software Package. In D. Behrend, K. D. Baver, and K. L. Armstrong, editors, *IVS 2016 General Meeting Proceedings: "New Horizons with VGOS"*, NASA/CP-2016-219016, 217–221, 2016.
2. J. Böhm, S. Böhm, J. Boisits, A. Girdiuk, J. Gruber, A. Hellerschmied, H. Krásná, D. Landskron, M. Madzak, D. Mayer, J. McCallum, L. McCallum, M. Schartner, K. Teke. Vienna VLBI and Satellite Software (VieVS) for Geodesy and Astrometry. *Publications of the Astronomical Society of the Pacific*, 130(986):044503, 2018 <https://doi.org/https://doi.org/10.1088/1538-3873/aaa22b>.
3. R. Dach, I. Selmke, A. Villiger, D. Arnold, L. Prange, S. Schaer, D. Sidorov, P. Stebler, A. Jäggi, U. Hugentobler. Review of recent GNSS modelling improvements based on CODEs Repro3 contribution. *Advances in Space Research*, 68:3, 1263–1280, 2021, <https://doi.org/10.1016/j.asr.2021.04.046>.
4. H. Hellmers, S. Modiri, S. Bachmann, D. Thaller, M. Blossfeld, M. Seitz, J. Gipson. Combined IVS contribution to the ITRF2020. *To appear in: IAG Symposia Series*, IAG Scientific Assembly 2021, 2022.
5. A.-S. Kirkvik, G.A. Hjelle, M. Dähnn, I. Fausk, E. Myssen. Where - A New Software for Geodetic Analysis. In R. Haas, S. García-Espada and J. A. L. Fernández, editors, *Proceedings of the 23rd European VLBI Group for Geodesy and Astrometry Working Meeting*, 248–252, 2017. doi:10.7419/162.08.2019.
6. Y. Kwak, M. Gerstl, M. Bloßfeld, D. Angermann, R. Schmid, M. Seitz. DOGS-RI: new VLBI analysis software at DGFI-TUM, *Proceedings of the 23rd European VLBI Group for Geodesy and Astrometry Working Meeting*, 212–215, 2017. doi:10.7419/162.08.2019.
7. D. Thaller, M. Krügel, M. Rothacher. Combining one year of homogeneously processed GPS, VLBI and SLR data. In: H. Drewes (ed), *Proceedings of the IAG Symposium on Geodetic Reference Frames GRF2006*, Munich, Germany. IAG Symposia, Vol. 134, Springer-Verlag, 17–22, 2006, doi:10.1007/978-3-642-00860-3\_3.